

# Performance optimization of resonant cavity enhanced *n*-GaAs homojunction far-infrared detectors: A theoretical study

M. M. Zheng, Y. H. Zhang,<sup>a)</sup> and W. Z. Shen

*Department of Physics, Laboratory of Condensed Matter Spectroscopy and Opto-Electronic Physics, Shanghai Jiao Tong University, 1954 Hua Shan Road, Shanghai 200030, People's Republic of China*

(Received 21 January 2009; accepted 11 March 2009; published online 27 April 2009)

The *n*-GaAs homojunction interfacial workfunction internal photoemission (HIWIP) far-infrared (FIR) detector is investigated to improve the quantum efficiency by simulation. The main structure, the bottom mirror, and the top mirror for the resonant cavity enhanced detector are optimized step by step. Two designs of the bottom mirror are suggested and compared. One consists of a bottom contact layer and one period of undoped/doped GaAs layers; the other is composed of a bottom contact layer, an undoped GaAs layer, and a gold layer. The results show that both mirrors enhance the quantum efficiency significantly and the gold mirror seems to be a better choice if not considering the technical difficulty. Preliminary study of the top mirror is also conducted. The top mirror shows a satisfactory effect under the condition that the reflectivity of the bottom mirror is high enough. The resulting quantum efficiency can be as high as 29.0% theoretically, which is much higher than *p*-GaAs and Si HIWIP FIR that was ever reported. © 2009 American Institute of Physics. [DOI: 10.1063/1.3116726]

## I. INTRODUCTION

High performance far-infrared (FIR) semiconductor detectors are becoming increasingly important for space astronomy applications.<sup>1</sup> In recent years, a homojunction interfacial workfunction internal photoemission (HIWIP) FIR semiconductor detector consisting of several periods of highly doped emitter layers and undoped intrinsic layers has attracted considerable attention because of its unique feature of tailorable cutoff wavelength (from several tens to a few hundreds of microns).<sup>2</sup> The detection mechanism involves FIR absorption in the highly doped emitter layers mainly by free carrier absorption followed by the internal photoemission of photoexcited carriers across the junction barrier and then collection. Although the quantum efficiency of HIWIP detector is limited by the internal photoemission mechanism, the advantages provided by the mature material technology for large scale focal plane arrays make HIWIP detector a favorable alternative in FIR applications. Significant progress has already been achieved in the development of both *p*-GaAs and Si HIWIP detectors,<sup>3–8</sup> which have the performance comparable to conventional Ge FIR photoconductors<sup>9</sup> and Ge blocked-impurity-band FIR detectors.<sup>10</sup> The recent rapid development of GaAs based long-wavelength quantum-well focal plane array cameras makes GaAs a promising candidate for developing HIWIP FIR detectors. However, up to now, most of the investigation on GaAs HIWIP FIR detectors was focused on *p*-GaAs,<sup>5</sup> and *n*-GaAs HIWIP FIR detectors have not been systematically studied yet, including the basic optimization of detector parameters.

In fact, though the theoretical analysis of performance of all HIWIP detectors is quite similar only with some modifi-

cations, *n*-GaAs HIWIP FIR detectors show some interesting features in contrary to *p*-GaAs HIWIP detectors because of the very small effective mass of carrier. For example, *n*-GaAs could acquire the same cutoff wavelength with lower doping concentration and is preferable for a long cutoff wavelength detector design due to the very small electron density of state mass.<sup>11</sup> It is known that high doping concentration will degrade the interface abruptness due to the strong space charge effect and limit the detector's performance (e.g., high dark current, low detectivity, etc.). In addition, higher mobility of *n*-GaAs leads to higher gain of detectors. In general, *n*-GaAs HIWIP FIR detector has some advantages over *p*-GaAs detector and needs to be studied in detail. We once investigated an *n*-GaAs HIWIP FIR detector roughly and tried to increase the quantum efficiency by applying a bottom mirror.<sup>12</sup> The highest absorption probability in the detector cavity is only 10.7%, resulting in a very low quantum efficiency, which is far from satisfaction and cannot meet the demand of practical use. It is known that quantum efficiency is a key parameter to characterize the performance of detectors. Low quantum efficiency will impede practical use of detectors. Therefore, one of the primary goals of the HIWIP FIR detector development is to increase the quantum efficiency as high as possible. A detailed optimization of *n*-GaAs HIWIP FIR detector to obtain high quantum efficiency is urgently needed.

Compared with the investigation on actual devices, it costs less time and money and is more convenient to optimize a device by simulation. Moreover, above all, it has been proved to be effective and accurate to simulate the performance of HIWIP FIR detector in terms of the previous research.<sup>12</sup> In this paper, the effect of material and structure parameters of *n*-GaAs HIWIP FIR detector on the quantum efficiency is analyzed in detail. We first optimize the main structure of *n*-GaAs HIWIP detector, and all the optimized

<sup>a)</sup>Author to whom correspondence should be addressed. Electronic mail: yuehzhang@sjtu.edu.cn. FAX: 86 21 54741040.

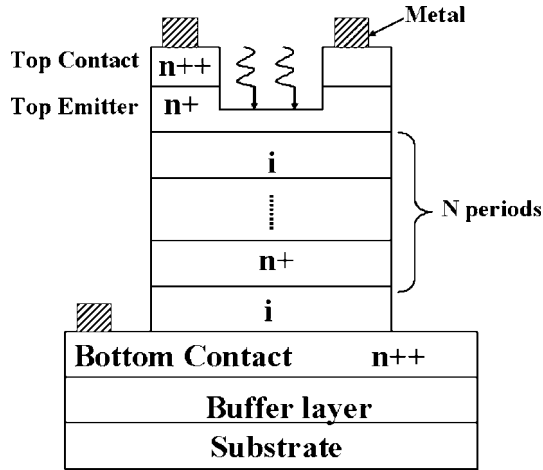


FIG. 1. The schematic structure of  $n$ -GaAs HIWIP FIR detector after device processing.  $n^{++}$ ,  $n^+$ , and  $i$  denote the contact layer, emitter layer, and intrinsic layer, respectively. The optical window is opened on the top.

parameters are presented. Then the influence of the bottom mirror of resonant cavity enhanced (RCE)  $n$ -GaAs HIWIP detector is discussed by proposing two kinds of different bottom mirrors. Finally, the top mirror is investigated and some concluding remarks and discussions are presented.

## II. RESULTS AND DISCUSSION

### A. Optimization of the main structure of detector

The schematic structure of the  $n$ -GaAs HIWIP FIR detector after device processing is illustrated in Fig. 1, in which the following calculation is based. It mainly consists of  $N$  periods of heavily doped emitter layers (with the thickness of  $d_e$  and the concentration of  $N_e$ ) and undoped intrinsic layers (with the thickness of  $d_i$ ). An optical window should be opened on the top for front side illumination, leaving around 100 nm top emitter layer within the window. To ensure ideal Ohmic contact, the doping concentration of the top and bottom contact layers should be much larger than the Mott transition concentration. Usually  $2 \times 10^{18} \text{ cm}^{-3}$  is preferred. Considering the demand of etch technology, the thickness of the bottom contact layer is assumed to be 500 nm. To compare with the result in Ref. 12, all the following results are calculated at  $\lambda = 60 \mu\text{m}$  if not pointed out specially.

All the theoretical analysis of performance of  $p$ -GaAs and Si HIWIP detectors can be applied to  $n$ -GaAs with some modifications. According to the detection mechanism of HIWIP detectors mentioned above, the quantum efficiency  $\eta$  should be the product of the photon absorption probability  $A$ , internal quantum efficiency  $\eta_b$ , and barrier collection efficiency  $\eta_c$ , giving the formula  $\eta = A \eta_b \eta_c$ . The photon absorption probability in the detector cavity is calculated in terms of the Fresnel matrix method. In the calculation, one simplification is made that the light is normally incident without considering any light polarization effects. The internal quantum efficiency  $\eta_b$  can be estimated, taking into account the inelastic scattering loss  $\eta_b = \exp(-d_e/L_z)$ , where  $L_z$  is the constant inelastic scattering mean free path.<sup>5</sup> Due to the low hot electron energy in FIR absorption and the very low operation temperature of  $n$ -GaAs HIWIP detector,  $L_z$  is esti-

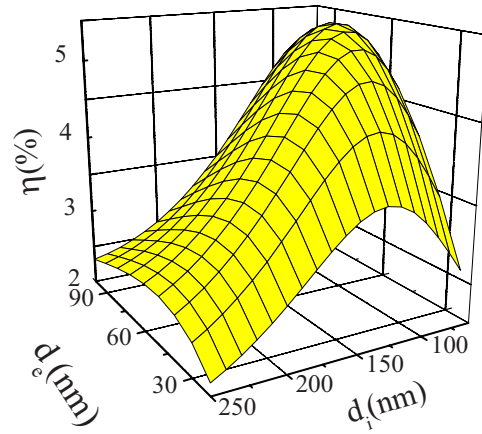


FIG. 2. (Color online) The dependence of the quantum efficiency  $\eta$  on the emitter thickness  $d_e$  and the intrinsic thickness  $d_i$  at  $60 \mu\text{m}$ .

mated to be  $725\text{--}800 \text{ \AA}$ .<sup>13</sup> In the calculation,  $L_z$  is determined as  $750 \text{ \AA}$ . The barrier collection efficiency  $\eta_c$  is given by  $\eta_c = \exp(-x_m/L_s)$ , where  $x_m = \sqrt{q/16\pi\epsilon_0\epsilon_s F}$  is the distance from the interface to the barrier maximum,  $F$  is the electric field in the intrinsic layer, and  $L_s$  is the electron scattering length in the undoped intrinsic layer. It is noted that the barrier collection efficiency can be enhanced even up to 100% by increasing the electric field.<sup>14</sup> Consequently, we will not discuss the effect of  $\eta_c$  since it does not involve any parameters related to our study, that is to say, we will just focus on  $\eta = A \eta_b$ ; the barrier collection efficiency is assumed to be 100%, which corresponds to the maximum quantum efficiency ( $\eta_c = 1$ ) of the HIWIP FIR detectors.

The main parameters that should be optimized include  $d_e$ ,  $d_i$ ,  $N_e$ , and  $N$ . It is known that high quantum efficiency can be acquired either by enhancing the photon absorption probability or by improving the internal photoemission probability of carriers. There are two kinds of effective way to enhance the photon absorption, i.e., increasing the total effective thickness and the absorption coefficient of the absorption layer (emitter layer). Previous research showed that a proper number of period are helpful to increase the effective absorption thickness and possible photocurrent gain.<sup>2</sup> However, the number of multilayer cannot be increased indefinitely. The period number should be less than 20 for  $n$ -GaAs HIWIP detectors according to simple estimation.<sup>15</sup> So to obtain the photon absorption as high as possible,  $N = 20$  is determined at first. According to the calculation, the absorption coefficient of  $n$ -GaAs in FIR region increases with increasing doping concentration, which is similar to the case of  $p$ -GaAs and Si.<sup>5,7</sup> Therefore, high doping concentration of the emitter layer could improve the FIR absorption of detector. Considering the detection mechanism of type II  $n$ -GaAs HIWIP detector, the doping concentration should fall in the scope of  $1.41 \times 10^{16} \text{ cm}^{-3} < N_e < 1.5 \times 10^{17} \text{ cm}^{-3}$ .<sup>16</sup> In the following simulation, the doping concentration of emitter layer is assumed to be  $1.2 \times 10^{17} \text{ cm}^{-3}$ , which corresponds to the cutoff wavelength of  $282 \mu\text{m}$  theoretically.<sup>11</sup> The remaining parameters that should be optimized are the thicknesses of the emitter and intrinsic layers. Figure 2 shows the dependence of the quantum efficiency on the thickness of the emitter and intrinsic layers. It is seen that

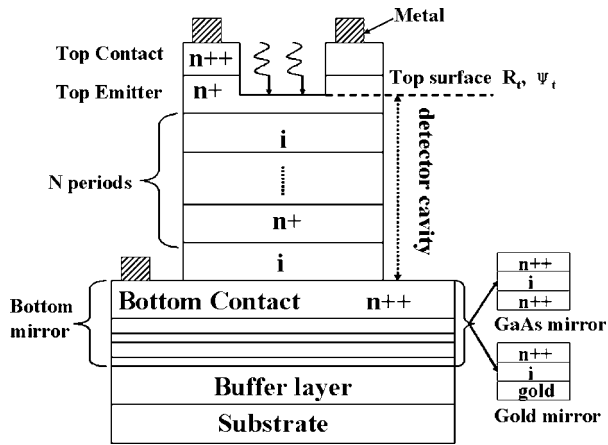


FIG. 3. The schematic structure of RCE  $n$ -GaAs HIWIP FIR detector after device processing. The whole detector can be divided into two parts: the detector cavity and the bottom mirror. Two different designs of bottom mirror are presented. The GaAs mirror consists of a bottom contact layer and one period of undoped/doped GaAs layers, while the gold mirror is composed of a bottom contact layer, an undoped GaAs layer, and a gold layer. The top mirror surface is characterized by the top mirror reflectivity  $R_t$  and phase shift  $\psi_t$ .

at a random  $d_i$ ,  $\eta$  always increases at first and then decreases. This is because increasing the thickness of the emitter layer leads to high absorption probability to some extent but decreases the internal quantum efficiency. So the ideal  $d_e$  is obtained by the tradeoff of photoabsorption probability and internal quantum efficiency. The thickness of the intrinsic layer determines the position of the emitter layer in the internal optical field directly and affects the total absorption thereby. It is expected that the emitter is placed at the maximum optical electric field of the standing wave formed inside the structure. Thus the optimum  $d_e$  and  $d_i$  are 60 and 100 nm, respectively, when the highest quantum efficiency is 4.9% and the corresponding absorption probability is 11.3%. In comparison with the absorption probability of 3.4% for the previous  $n$ -GaAs HIWIP detector without a bottom mirror in Ref. 12, the absorption probability is two times higher. Now all the optimized parameters of  $n$ -GaAs HIWIP detector are obtained:  $N=20$ ,  $N_e=1.2 \times 10^{17} \text{ cm}^{-3}$ ,  $d_e=60 \text{ nm}$ , and  $d_i=100 \text{ nm}$ .

## B. Discussion of the bottom mirrors

Though the absorption probability is increased significantly, the total quantum efficiency is still relatively low and needs to be further improved. Generally, applying a resonant cavity to a detector is a common choice to increase the quantum efficiency. The structure of RCE detectors is formed by sandwiching detectors between a pair of mirrors. Figure 3 presents the sketch of the RCE detector structure for simulation. At the first step of the design of resonant cavity structure, the top mirror of the RCE detector will not be considered for simplicity and is assumed to be the native semiconductor and air interface. We will focus on discussing the bottom mirror. It is clear that the whole RCE detector structure mainly consists of two parts, the basic detector cavity and the bottom mirror, which are separated by the interface between the bottom intrinsic layer and bottom contact

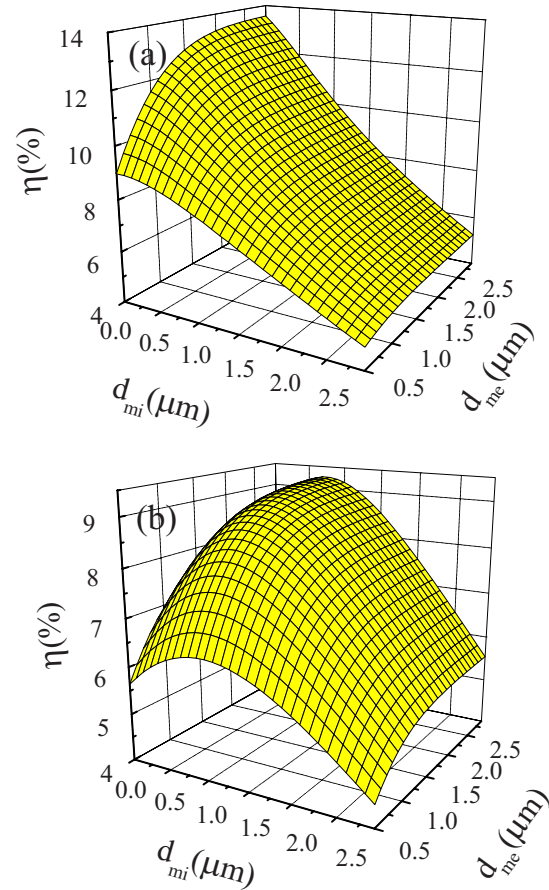


FIG. 4. (Color online) The dependence of quantum efficiency  $\eta$  on the thicknesses of the undoped and doped GaAs layers in the bottom mirror for (a) the optimized detector structure and (b) the detector with  $N=15$ .

layer. Only the photon absorption in the detector cavity contributes to the quantum efficiency. Thus, the quantum efficiency calculated in the following is just the one in the detector cavity.

Aiming at a given  $n$ -GaAs HIWIP FIR detector, a kind of bottom mirror was once proposed in our previous work, which was composed of the bottom contact layer and one period of undoped/doped GaAs layers lying below, as depicted in Fig. 3. This kind of bottom mirror design has been proved useful to improve the absorption probability for both the  $p$ -type<sup>17</sup> and  $n$ -type GaAs HIWIP detectors.<sup>12</sup> Such design will also be applied to the above optimized  $n$ -GaAs HIWIP detector firstly. To obtain the high interface reflectivity of bottom mirror, the doping concentration of doped  $n$ -GaAs layer is determined to be  $3.0 \times 10^{18} \text{ cm}^{-3}$ , considering the amphoteric behavior and self-compensation caused by high doping concentration.<sup>18</sup> Figure 4(a) shows the dependence of  $\eta$  in the detector cavity on the thicknesses of the undoped ( $d_{mi}$ ) and doped ( $d_{me}$ ) GaAs layers in the bottom mirror. It is noted that the absorption probability increases with decreasing  $d_{mi}$ , while it increases with increasing  $d_{me}$  and gradually saturates when  $d_{me}$  is more than 1800 nm. Therefore, the optimum values for  $d_{mi}$  and  $d_{me}$  are 0 and 1800 nm, respectively, when the corresponding quantum efficiency is 13.2% that is about two times higher than that of the detector (4.9%) without a bottom mirror. It is noted that when  $d_{mi}$  is zero, it indicates that the optimized bottom mir-

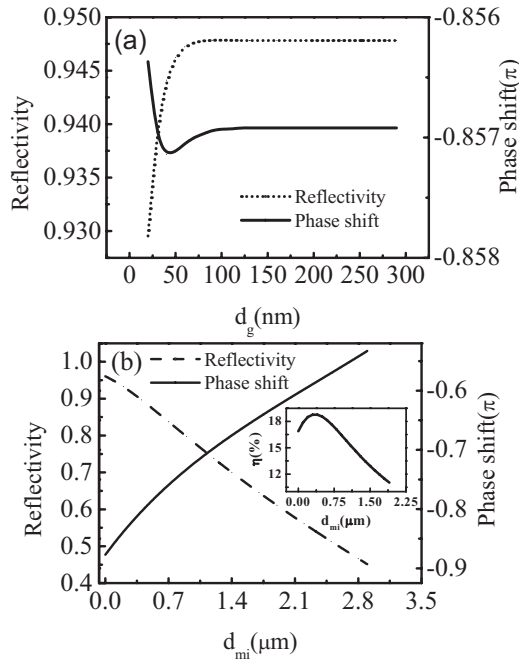


FIG. 5. The reflectivity and phase shift of the bottom mirror vs the thickness of (a) the gold layer  $d_g$  and (b) the undoped GaAs layer  $d_{mi}$ . The inset displays dependence of the quantum efficiency  $\eta$  on  $d_{mi}$ .

ror is just composed of heavily doped contact layer. This is only a specific example corresponding to the case that the main structure of the detector is best optimized. For the case of the detector structure with other nonoptimized parameters, the optimized  $d_{mi}$  in the bottom mirror is not always zero. For example, if the detector has the period number  $N=15$ , the optimized  $d_{mi}$  should be 700 nm, as displayed in Fig. 4(b), which is also the case of the detector with other main structure parameters.

Due to the high reflectivity, metal has also been applied to serve as a perfect mirror for the near-infrared<sup>19</sup> and the midinfrared photodetectors.<sup>20</sup> This design of bottom mirror has been proved feasible technically to improve the peak quantum efficiency significantly for the RCE GaAs/AlGaAs quantum-well infrared photodetectors.<sup>21</sup> Therefore, it is natural to try employing a metal layer to the bottom mirror of HIWIP detector. Due to the excellent reflection characteristic, gold is usually the best candidate, with the refractive index  $N_{Au}=152+329i$  at the wavelength of  $67\ \mu\text{m}$ .<sup>22</sup> Such bottom mirror composed of a bottom contact layer, an undoped GaAs layer, and a gold layer, as shown in Fig. 3, is investigated. The realization of the reflectivity and phase shift of the bottom mirror of a resonant cavity is usually necessary. Figure 5(a) displays the dependence of the reflectivity and phase shift on the thickness of gold layer  $d_g$ . It is clear that  $d_g$  has little influence on reflectivity and phase shift from the fact that reflectivity varies from 0.930 to 0.956, and the phase shift varies from  $-0.857\pi$  to  $-0.856\pi$  when  $d_g$  changes from 40 to 300 nm. It is also found that both reflectivity and phase shift are independent of  $d_g$  when  $d_g$  is more than 100 nm. This may be ascribed to the small skin depth of the gold layer. Consequently,  $d_g$  is considered to be 100 nm in further calculation. In contrast to the case of the gold layer, the thickness of the undoped GaAs layer  $d_{mi}$  affects the

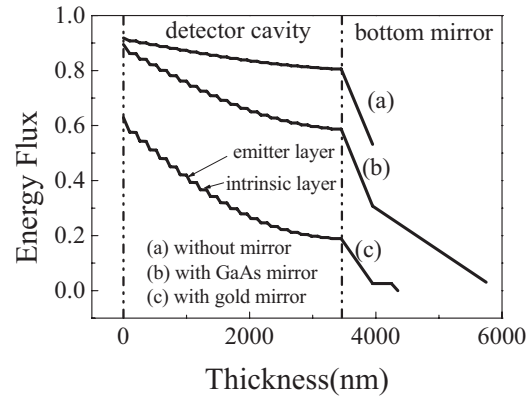


FIG. 6. The energy flux distribution from the top layer to the bottom layer for (a) the detector without bottom mirror, (b) the RCE detector with GaAs mirror, and (c) the RCE detector with gold mirror. The thickness of zero denotes the native semiconductor and air interface.

reflectivity and phase shift of the bottom mirror significantly, which in fact determines the position of the gold layer, as shown in Fig. 5(b). It is well known that good absorption in the detector cavity requires not only high reflectivity but also well matched phase shift of mirrors. Therefore, the choice of  $d_{mi}$  is based on the tradeoff between the reflectivity and phase shift. The direct relationship between the quantum efficiency and  $d_{mi}$  is displayed in the inset in Fig. 5(b). The curve indicates that the optimum thickness of  $d_{mi}$  is 300 nm when the bottom mirror reflectivity is 0.92 and when the phase shift is  $-0.82\pi$ . The ultimate quantum efficiency is 18.8%, which is almost four times as high as that of the detector without bottom mirror (4.9%) and is much higher than that of  $p$ -GaAs and Si HIWIP detector that was ever reported.

### C. Contrast of the two designs of the bottom mirror

Up to now, two kinds of designs of the bottom mirror have been demonstrated. For convenience of comparison, we temporarily name them as the GaAs mirror and the gold mirror, separately. Better understanding of the photon absorption of each layer in the total detector is helpful to investigate the effect of such two bottom mirrors. The calculation of energy flux provides a direct and clear approach to demonstrate the absorption in every layer. Figure 6 shows the energy flux from the top layer to the bottom layer of three detector samples, i.e., (a) the detector without bottom mirror, (b) the RCE detector with GaAs mirror, and (c) the RCE detector with gold mirror. In fact, the slope of the curve describes the efficiency of the absorption. It is clear that the main features are similar for the three samples, which show the ladderlike absorption, and the absorption in the intrinsic layer is nearly negligible in contrast to that of the doped layers. Though the parameters of detector cavity structure are the same, the absorption in this segment is quite different. It is low for the detector without a bottom mirror, and most of the optical energy flows out of the sample. However, due to the restriction effect of the resonant cavity by forming the standing wave, the absorption in the detector cavity is high for the detector with bottom mirrors. Comparing the two RCE detectors, the absorption in the detector cavity of the RCE de-

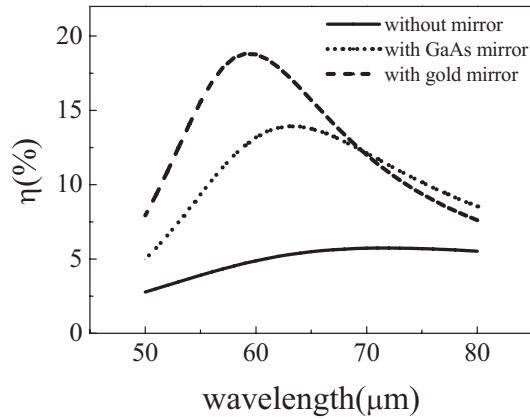


FIG. 7. The dependence of quantum efficiency  $\eta$  on wavelength for the detector without bottom mirror, with GaAs mirror, and with gold mirror.

detector with gold mirror is enhanced more significantly than that in the RCE detector with GaAs mirror, which may be caused by two reasons. On one hand, this is ascribed to higher reflectivity (i.e., 0.92 for gold mirror and 0.64 for GaAs mirror) enhancing the resonant cavity effect. On the other hand, this is a result of the lower absorption of the bottom mirror itself due to the smaller skin depth of gold layer compared with the heavily doped GaAs layer in GaAs mirror.

To know the performance of detectors over the broad wavelength coverage, the quantum efficiency at other wavelength besides 60  $\mu\text{m}$  for the three cases is calculated in Fig. 7. Unlike the typical RCE detector in the near-infrared region,<sup>19</sup> the RCE HIWIP FIR detector does not show strong wavelength selectivity. In a wide wavelength scope including the selected wavelength of 60  $\mu\text{m}$ , the bottom mirrors demonstrate excellent effect, making the quantum efficiency improve obviously. In general, from the view point of the quantum efficiency, the total thickness of the bottom mirror, and the broad wavelength characteristics, the gold mirror seems to be a better choice if not considering the difficulty of process technique,<sup>21</sup> whereas the GaAs mirror is simpler to obtain technically.

#### D. Discussion of the top mirror

The bottom mirror has been discussed in detail. However, the top mirror has not been considered yet, which was assumed to be the interface between the air and the native semiconductor. As we know, an appropriate top mirror that is matched to the bottom mirror may further increase the quantum efficiency in the detector cavity. In the following, a preliminary study will be conducted to investigate the top mirror.

It is convenient to regard the top mirror as a nonabsorbing interface with reflectivity  $R_t$  and phase shift  $\psi_t$  at the top of the resonant cavity. In order to further improve the quantum efficiency, top mirrors with different  $R_t$  and  $\psi_t$  should be selected for the RCE detector with GaAs and gold mirrors, as displayed in Fig. 8. For such two cases, the main features are similar, i.e., at a random given  $R_t$ , the highest  $\eta$  occurs at a certain  $\psi_t$ , which we name as the resonant phase shift. For

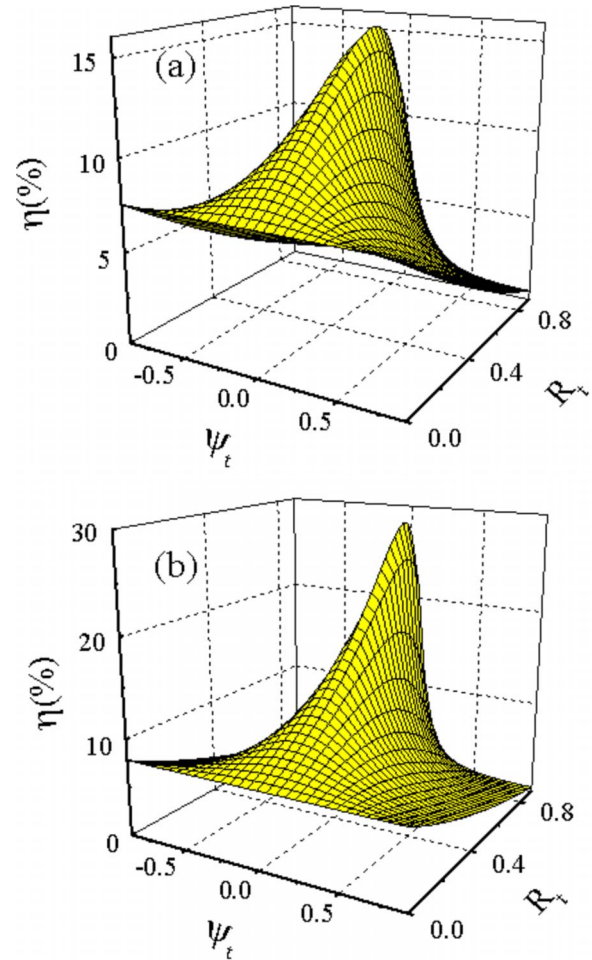


FIG. 8. (Color online) The dependence of quantum efficiency  $\eta$  on the top mirror reflectivity  $R_t$  and phase shift  $\psi_t$  for the detector (a) with the GaAs mirror and (b) with the gold mirror.

the RCE detector with GaAs mirror, the resonant parameter is  $R_t=0.52$ , and  $\psi_t=-0.07\pi$ . As a result, the corresponding quantum efficiency is 15.6%, which is only a little higher than that of 13.2% before applying the top mirror. In contrast, for the RCE detector with gold mirror, when the reflectivity and phase shift of top mirror are 0.72 and  $0.01\pi$ , the maximum calculated quantum efficiency reaches 29.0%, which is enhanced greatly than that of 18.8% without the top mirror, meeting the stringent requirement of NASA's SIRT program.<sup>23</sup> This may have resulted from the higher reflectivity of the gold mirror, in which the bottom mirror reflectivity  $R_b$  is 0.92 and phase shift  $\psi_b$  is  $-0.82\pi$ . In order to verify this assumption, the dependence of  $\eta$  on  $R_t$  assuming different bottom mirror reflectivities is investigated in Fig. 9, considering the condition when the bottom mirror phase shift is  $-0.82\pi$  and when the matched phase shift of top mirror is  $0.01\pi$  (both of the top and the bottom mirrors are at the resonant phase shift). It is noted that the higher the  $R_b$  is, the stronger dependence of  $\eta$  has on  $R_t$ , and the highest  $\eta$  occurs at certain  $R_t$  for a given  $R_b$ . The quantum efficiency is almost insensitive to  $R_t$  when  $R_b$  is low, such as  $R_b=0.49$ . This indicates that only when the reflectivity of the bottom mirror is high enough, it is meaningful to design the top mirror. Therefore, there is more potential to optimize the top mirror for the

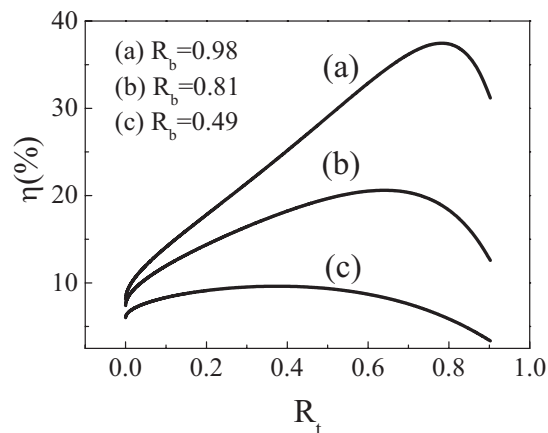


FIG. 9. The dependence of quantum efficiency  $\eta$  on top mirror reflectivity  $R_t$  for bottom mirror reflectivity  $R_b=0.49, 0.81,$  and  $0.98$ . The top mirror phase shift  $\psi_t$  is  $0.01\pi$  and the bottom mirror phase shift  $\psi_b$  is  $-0.82\pi$ .

detector with gold mirror due to higher reflectivity. Further research will be focused on designing the top mirror of the RCE  $n$ -GaAs HIWIP with gold mirror, such as the antireflection coating.

### III. CONCLUSION

In this paper, the optimization of the RCE  $n$ -GaAs HIWIP detector including the main structure, the bottom mirror, and the top mirror was conducted to improve the quantum efficiency. Two designs of the bottom mirror (GaAs mirror and gold mirror) were proposed and investigated. It has been shown that significant enhancement in quantum efficiency can be obtained by applying both kinds of mirrors. The resulting quantum efficiency of the RCE detector with gold mirror is 18.8%, which is larger than those of the  $p$ -GaAs and Si HIWIP FIR detectors that was ever reported. Due to higher reflectivity and better broad wavelength characteristic, the gold mirror seems to be a better choice if not considering the technical challenge. In addition, the matched top mirror for  $n$ -GaAs HIWIP has also been discussed in this paper. We find that only when the reflectivity of bottom mirror is high enough, it is meaningful to design a top mirror. The reason-

able design of the top mirror may make the quantum efficiency of the RCE  $n$ -GaAs HIWIP detector reach 29.0%, meeting the requirement of NASA's SIRT program.

### ACKNOWLEDGMENTS

This work is supported in part by the Natural Science Foundation of China under Contract Nos. 10774100 and 10304010 and the Minister of Education of PCSIRT (Contract No. IRT0524).

- <sup>1</sup>M. W. Werner, *Infrared Phys. Technol.* **35**, 539 (1994).
- <sup>2</sup>A. G. U. Perera, in *Physics of Thin Films*, edited by M. H. Francombe and J. L. Vossen (Academic, New York, 1995), Vol. 21, pp. 1–75.
- <sup>3</sup>A. G. U. Perera, H. X. Yuan, S. K. Gamage, W. Z. Shen, M. H. Francombe, H. C. Liu, M. Buchanan, and W. J. Schaff, *J. Appl. Phys.* **81**, 3316 (1997).
- <sup>4</sup>A. G. U. Perera and W. Z. Shen, *Opto-Electron. Rev.* **7**, 153 (1999).
- <sup>5</sup>W. Z. Shen, A. G. U. Perera, H. C. Liu, M. Buchanan, and W. J. Schaff, *Appl. Phys. Lett.* **71**, 2677 (1997).
- <sup>6</sup>H. X. Yuan and A. G. U. Perera, *Appl. Phys. Lett.* **66**, 2262 (1995).
- <sup>7</sup>A. G. U. Perera, W. Z. Shen, H. C. Liu, M. Buchanan, M. O. Tranner, and K. L. Wang, *Appl. Phys. Lett.* **72**, 2307 (1998).
- <sup>8</sup>A. G. U. Perera, W. Z. Shen, W. C. Mallard, M. O. Tanner, and K. L. Wang, *Appl. Phys. Lett.* **71**, 515 (1997).
- <sup>9</sup>J. W. Berman and E. E. Haller, *Infrared Phys. Technol.* **35**, 827 (1994).
- <sup>10</sup>D. M. Watson, M. T. Guptill, J. E. Huffman, T. N. Krabach, S. N. Raines, and S. Satyapal, *J. Appl. Phys.* **74**, 4199 (1993).
- <sup>11</sup>H. T. Luo, W. Z. Shen, Y. H. Zhang, and H. F. Yang, *Physica B* **324**, 379 (2002).
- <sup>12</sup>Y. H. Zhang, H. T. Luo, and W. Z. Shen, *Appl. Phys. Lett.* **82**, 1129 (2003).
- <sup>13</sup>B. Y.-K. Hu and S. D. Sarma, *Phys. Rev. B* **44**, 8319 (1991).
- <sup>14</sup>W. Z. Shen and A. G. U. Perera, *J. Appl. Phys.* **83**, 3923 (1997).
- <sup>15</sup>A. G. U. Perera, J.-W. Choe, M. H. Francombe, R. E. Sheriff, and R. P. Devaty, *Superlattices Microstruct.* **14**, 123 (1993).
- <sup>16</sup>A. G. U. Perera, H. X. Yuan, and M. H. Francombe, *J. Appl. Phys.* **77**, 915 (1995).
- <sup>17</sup>Y. H. Zhang, H. T. Luo, and W. Z. Shen, *Eur. Phys. J.: Appl. Phys.* **22**, 165 (2003).
- <sup>18</sup>G. Borghs, K. Bhattacharyya, K. Deneffe, P. V. Mieghem, and R. Mertens, *J. Appl. Phys.* **66**, 4381 (1989).
- <sup>19</sup>M. Casalino, L. Sirlito, L. Moretti, M. Gioffrè, G. Coppola, and I. Rendina, *Appl. Phys. Lett.* **92**, 251104 (2008).
- <sup>20</sup>M. Arnold, D. Zimin, and H. Zogg, *Appl. Phys. Lett.* **87**, 141103 (2005).
- <sup>21</sup>A. Shen, H. C. Liu, M. Gao, E. Dupont, and M. Buchanan, *Appl. Phys. Lett.* **77**, 2400 (2000).
- <sup>22</sup>M. A. Ordal, L. L. Long, R. J. Bell, S. E. Bell, R. R. Bell, R. W. Alexander, Jr., and C. A. Ward, *Appl. Opt.* **22**, 1099 (1983).
- <sup>23</sup>E. T. Young, *Proc. SPIE* **2019**, 96 (1993).